

Label-free imaging by stimulated parametric emission microscopy reveals a difference in hemoglobin distribution between live and fixed erythrocytes

Hieu M. Dang,^{a,†} Gen Omura,^{b,†} Toshiyuki Umano,^a Masatomo Yamagiwa,^b Shin'ichiro Kajiyama,^{a,b} Yasuyuki Ozeki,^b Kazuyoshi Itoh,^b and Kiichi Fukui^{a,*}

^aOsaka University, Graduate School of Engineering, Department of Biotechnology,
^bDepartment of Material and Life Science, 2-1 Yamadaoka, Suita, Osaka 565-0871, Japan

Abstract. We demonstrate that stimulated parametric emission (SPE) microscopy enables label-free, 3-D visualization of internal hemoglobin distribution of live mouse and chicken erythrocytes with high sensitivity. Change in hemoglobin distribution in chicken erythrocytes before and after ethanol fixation is clearly visualized. © 2009 Society of Photo-Optical Instrumentation Engineers. [DOI: 10.1117/1.3207151]

Keywords: stimulated parametric emission; hemoglobin; unstained; nonlinear microscopy; three dimensional.

Paper 09089LRR received Mar. 18, 2009; revised manuscript received Jun. 15, 2009; accepted for publication Jun. 30, 2009; published online Aug. 25, 2009.

Hemoglobin is the primary constituent of erythrocytes and its change in concentration is linked to various kinds of diseases from anemia to polycythemia. Previous reports have studied the distribution of hemoglobin, both in the nucleus and cytoplasm of chicken erythrocytes,¹ and suggested its roles in various stages of erythrocyte development.^{2,3} However, fluorescence microscopy used in these studies are usually compromised by fixation artifacts that can be observed as intense perinuclear and marginal concentrations of hemoglobin in chicken erythrocytes.^{4,5} A live-cell imaging technique that provides intrinsic/label-free detection of hemoglobin is thus demanded.

Currently, great attention is being focused on nonlinear optical processes that provide endogenous signatures of not just hemoglobin, but biological materials generally. Previous reports have demonstrated that hemoglobin possesses large two-photon absorptivities and nonlinear resonances in the infrared region.^{6,7} A recent label-free technique called two-photon absorption (TPA) microscopy can image and differentiate between oxyhemoglobin and deoxyhemoglobin in tissue by direct detection of their two-photon absorption.^{8,9} Earlier, third-harmonic generation (THG) was also found to be effective

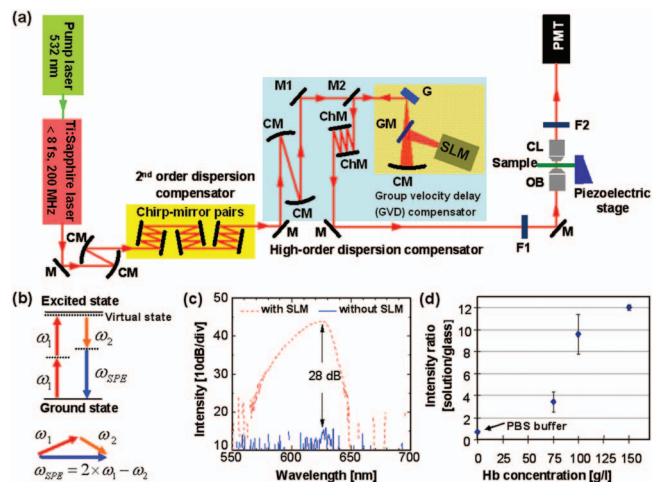


Fig. 1 (a) Schematic setup of SPE. OB, objective lens; CL, collector lens; M, mirror; F1, F2: sets of optical filters; SLM: spatial light modulator; G: grating; GM: rectangular gold mirror; CM: concave mirror; and ChM: chirped mirror. M1 and M2 are positioned in the same vertical plane but at different heights. M1 delivers the precompensated beam to the GVD compensator, while M2 receives and delivers the output beam, which will serve as an excitation beam to the microscopy. (b) Energy and phase matching diagrams of SPE. (c) Intensity diagram of SPE signal before and after dispersion compression by SLM. (d) Dependence of SPE signal on hemoglobin concentration.

for visualizing flowing erythrocytes, and was assumed to correlate with hemoglobin concentration.¹⁰ Recently, hemoglobin was found to provide a resonantly enhanced THG signal around 420 nm.¹¹ However, high-sensitivity THG imaging of hemoglobin seems difficult, since the generation of THG is usually allowed only at interfaces of different media.

We recently proposed stimulated parametric emission (SPE) microscopy for label-free visualization of biological samples based on electronics resonance of sample molecules.^{12,13} SPE is a nonlinear-optical four-wave mixing (FWM) process that involves the mixing of a pump beam at an angular frequency of ω_1 and a dump beam at ω_2 to produce a signal at frequency $\omega_{SPE} = 2 \times \omega_1 - \omega_2$. SPE has been described as a source of noise in coherent anti-Stoke Raman scattering (CARS) microscopy.¹⁴ However, with the use of a Ti:sapphire laser with a pulse-width shorter than 10 fs in a tightly focused condition, we suggested that SPE is dominant among the FWM processes, and the CARS signal is relegated to a source of noise in SPE.¹² Considering the relaxed phase matching condition in SPE as well as the large nonlinear absorptivities of hemoglobin, the SPE visualization of hemoglobin seems attractive and possible for high sensitivity.

Here, using a system modified from that previously proposed,¹² we report high-resolution imaging of unstained hemoglobin in live erythrocytes. The technique uses a mode-locked Ti:sapphire laser ($\lambda = 660$ to 930 nm) (Venteon I Pulse:One ≤ 8 fs, 200 MHz, Nanolayers, Rheinbreitbach, Germany) pumped by a continuous-wave laser (532 nm, Verdi-V10, Coherent, Palestine, Texas) [Fig. 1(a)]. One set of filters (F1) (SCF-50S-66R long-pass filter, Sigma-Koki, and Tokyo, Japan, SI0870 short-pass filter, Asahi Spectra, Torrance, California) placed in front of the objective lens (OB)

[†]These authors contributed equally to this study.

*Address all correspondence to: Kiichi Fukui; E-mail: kfukui@bio.eng.osaka-u.ac.jp

(100×, 1.4 NA, oil immersion, Olympus) and one set of filters (F2) (SV0780; SV0750 and SV0650 short-pass filters, Asahi Spectra) placed to the rear of the collector lens (CL) (100×, 0.8 NA, Olympus) not only provide an excitation beam with wavelengths ranging from 670 to 870 nm, but also restrict the SPE signal to the region from 570 to 650 nm and eliminate the remnants of the excitation beam from the signal. Due to the strong requirement for phase matching, two separate portions of the irradiation beam play pump and dump roles to produce SPE signals. Figure 1(b) shows energy and phase matching diagrams of SPE. The detector is a photomultiplier tube (PMT) (H7732, Hamamatsu Photonics).

The modifications, as mentioned, are mainly on the use of a single broadband laser and a spatial light modulation (SLM) embedded compensation system composed of two parts: a chirped mirror system precompensates for second-order dispersion and a group velocity delay (GVD) compensator compensates for higher order dispersion, indicated in Fig. 1(a) as yellow and aqua boxes, respectively. The GVD compensator consists of an optical grating (G) and the SLM, and its working has been described in detail previously.¹⁵ With the use of the embedded SLM in this modified system, the SPE signal intensity has effectively increased about 1000 times (~30 dB) [Fig. 1(c)]. As the SPE signal is proportional to the cubed laser power, the power can be reduced to about a tenth, or the sensitivity can be improved about ten-fold.

In this demonstration, we visualized hemoglobin in mouse and chicken erythrocytes. We confirmed that the SPE signal intensity of hemoglobin is dependent on its concentration [Fig. 1(d)]. Since the SPE process could be resonantly enhanced by the presence of a quantum level near $2 \times \omega_1$, the strong SPE signal of hemoglobin, presumably, originates from the two-photon resonance of hemoglobin. Proof of the existence of two-photon resonance is given in Fig. 1(d), although it is not sufficient enough. Further elucidation requires sophisticated nonlinear spectroscopic experiments in the future. As hemoglobin is a nonfluorescent protein, it is not necessary to care about signal contamination by hemoglobin fluorescence. In addition, we have measured the intracellular autofluorescences by inserting a polarizer to eliminate only the SPE signal. The experiment suggested that the contribution of fluorescence is as small as that from the culture medium (data not shown). 3-D imaging of a mouse erythrocyte [Fig. 2(a)] clearly illustrates the 3-D doughnut-shape distribution of hemoglobin inside the cells. Figure 2(b) shows an even distribution of hemoglobin in a mouse spherocyte, an erythrocyte with spherical cell morphology. Figures 2(c)–2(e) show different sectional images of the mouse erythrocyte at different z positions. The 0- μm z position [Fig. 2(e)] shows an increase in nonresonant background noise or a decrease in the signal-to-noise ratio as the focal plane moves out of the cell area. Further observations with chicken erythrocytes revealed a difference in hemoglobin distribution between fresh and ethanol-fixed cells. Hemoglobin in a fresh chicken erythrocyte is distributed evenly over the cytoplasm and nucleus [Fig. 2(f)], while in an ethanol-fixed cell, it is aggregated in the cytoplasm and close to the perinuclear region [Fig. 2(g) and Video 1]. Representative sectional images of the fixed cell are displayed in Figs. 2(h)–2(j). Figure 2(j) shows the intensity profile along the diagonal indicated by the yellow line of Fig. 2(h). It indicates that the enhancement factor between reso-

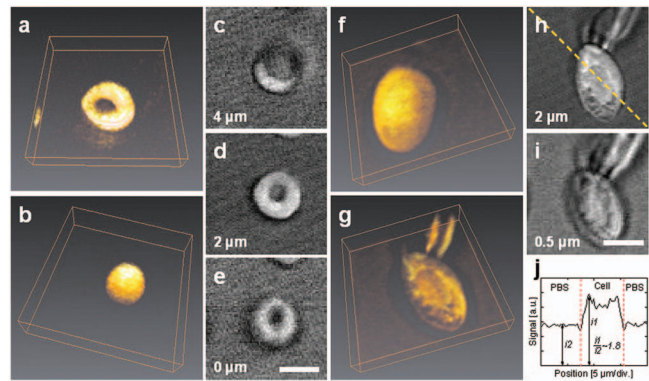
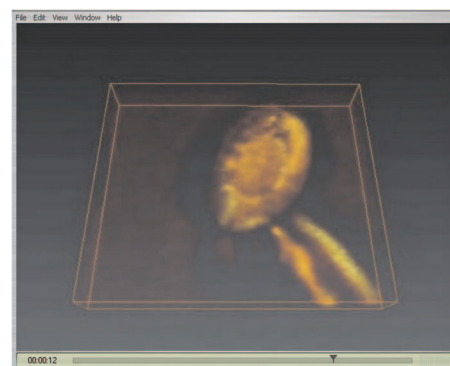


Fig. 2 (a) and (b) 3-D images of (a) a fresh mouse erythrocyte and (b) spherocyte (b) taken at 2-mW laser power. Images are constructed from nine and seven sectional images, respectively. Imaging conditions: 1-ms pixel dwell time, 0.2- μm x-y scanning-step, and 0.5- μm incremental step along the z axis. Box dimensions are $15 \times 15 \times 4 \mu\text{m}$ and $15 \times 15 \times 3 \mu\text{m}$, respectively. (c)–(e) Representative sectional images of the fresh mouse erythrocyte. (f) and (g) 3-D images of (f) fresh and (g) ethanol-fixed chicken erythrocytes taken at 2-mW laser power. Each image is constructed from six sectional images. Imaging condition: 1-ms pixel dwell time, 0.2- μm x-y scanning-step, and 0.5- μm incremental step along the z axis. Box dimensions are $15 \times 15 \times 2.5 \mu\text{m}$. (h) and (i) Representative sectional images of the fixed chicken erythrocyte. Bars: 5 μm . (j) Intensity profile along the yellow line in (h).

nantly enhanced and nonresonant signals can be as high as 1.8. This factor is much higher than the general SPE contrast of maximum 1.35 in other cases, in which we observed various kinds of biological materials in plant BY-2 and HeLa cells (data not shown).

The intense perinuclear hemoglobin concentration has been reported previously.^{4,5} It is shown that fixation methods such as paraformaldehyde could lead to obvious morphological changes, while cell morphology showed no significant changes by methanol fixations.¹⁶ Our observations of paraformaldehyde and ethanol-fixed chicken erythrocytes agree with this finding. Therefore, in the scope of this work, we placed our focus only on the exploitation of differences between live and ethanol-fixed chicken erythrocytes. This is



Video 1 Video shows vertical and horizontal 360-deg rotations of 3-D image of an ethanol-fixed chicken red blood cell. The image is constructed from a stack of six sectional images. Box dimensions are $15 \times 15 \times 2.5 \mu\text{m}$, (QuickTime, 2.83 Mb). [URL: <http://dx.doi.org/10.1117/1.3207151.1>].

the first time SPE has been introduced as a label-free technique for visualization of hemoglobin with a high sensitivity, and also the first illustration of hemoglobin distribution differences by means of using a label-free method. The 2-mW average laser power used in all observations is quite low in comparison with reported hemoglobin visualizations by THG and TPA.⁸⁻¹¹ Therefore, SPE could potentially be an alternative, effective, and direct way not only for studying clinical aspects of hemoglobin in erythrocytes, but also for biological and medical studies.

In conclusion, we have demonstrated that SPE can effectively visualize hemoglobin with high sensitivity and reveal its 3-D distribution in erythrocytes. Due to its ability to produce an enhanced intrinsic signal from hemoglobin, SPE demonstrates the difference in hemoglobin distribution between fresh and fixed chicken erythrocytes. Because SPE uses a single laser, it could readily be coupled with other multiphoton techniques, e.g., two-photon fluorescence, second-harmonic generation, or THG. We believe that SPE will soon find an important place in the field of biological and medical imaging. Future works could focus on improving the sensitivity and selectivity by using different sets of pump and probe pulses, or building a fast SPE system for monitoring rapid intracellular processes.

Acknowledgments

Dang thanks the Ministry of Education, Culture, Sports, Science and Technology, Japan (MEXT) and the International Graduate Program for Frontier Biotechnology, Graduate School of Engineering, Osaka University, for fellowship support. This work was supported in part by a grant from the Cooperative Link of Unique Science and Technology for Economy Revitalization promoted by MEXT to Fukui and Itoh. This work was also supported in part by a grant from the SENTAN, Japan Science and Technology Agency to Itoh and Fukui. Finally, Dang thanks Lim Xue Min for providing fresh mouse erythrocytes, Joyce Cartagena for providing fixed chicken erythrocytes, and the Kyowa Foods Company for providing live chickens for bleeding.

References

1. D. Kabat, "Organization of hemoglobin synthesis in chicken erythrocytes," *J. Biol. Chem.* **243**(10), 2597-2606 (1968).
2. J. Tooze and H. G. Davies, "The occurrence and possible significance of hemoglobin in the chromosomal regions of mature erythrocyte nuclei of the newt *Triturus cristatus cristatus*," *J. Cell Biol.* **16**, 501-511 (1963).
3. C. Baglioni, "Ontogenesis of erythrocytes and hemoglobin formation," *J. Cell Physiol.* **67**, 169-184 (1966).
4. S. Granick and R. D. Levere, "The intracellular localization of heme by a fluorescence technique," *J. Cell Biol.* **26**, 167-176 (1965).
5. B. R. A. O'Brien, "The present of hemoglobin within the nucleus of the embryonic chick erythroblast," *Exp. Cell Res.* **21**, 226-228 (1960).
6. G. O. Clay, A. C. Millard, C. B. Schaffer, J. Aus-der-Au, P. S. Tsai, J. A. Squier, and D. Kleinfeld, "Spectroscopy of third-harmonic generation: evidence for resonances in model compounds and ligated hemoglobin," *J. Biomed. Opt.* **23**(5), 932-950 (2006).
7. G. O. Clay, C. B. Shaffer, and D. Kleinfeld, "Large two-photon absorptivity of hemoglobin in the infrared range of 780-880 nm," *J. Chem. Phys.* **126**, 025102 (2007).
8. D. Fu, T. Ye, T. E. Matthews, B. J. Chen, G. Yurtserver, and W. S. Warren, "High-resolution *in vivo* imaging of blood vessels without labeling," *Opt. Lett.* **32**(18), 2641-2643 (2007).
9. D. Fu, T. E. Matthews, T. Ye, I. R. Piletic, and W. S. Warren, "Label-free *in vivo* optical imaging of microvasculature and oxygenation level," *J. Biomed. Opt.* **13**(4), 045031-045033 (2008).
10. A. C. Millard, P. W. Wiseman, D. N. Fittinghoff, K. R. Wilson, J. A. Squier, and M. Müller, "Third-harmonic generation microscopy by use of a compact, femtosecond fiber laser source," *Appl. Opt.* **38**(36), 7393-7397 (1999).
11. R. D. Schaller, J. C. Johnson, and R. J. Saykally, "Nonlinear chemical imaging microscopy: near-field third harmonic generation imaging of human red blood cells," *Anal. Chem.* **72**(21), 5361-5364 (2000).
12. K. Isobe, S. Kataoka, R. Murase, W. Watanabe, T. Higashi, S. Kawakami, S. Matsunaga, K. Fukui, and K. Itoh, "Stimulated parametric emission microscopy," *Opt. Express* **14**(2), 786-793 (2006).
13. K. Isobe, Y. Ozeki, T. Kawasumi, S. Kataoka, S. Kajiyama, K. Fukui, and K. Itoh, "Highly sensitive spectral interferometric four-wave mixing microscopy near the shot noise limit and its combination with two-photon excited fluorescence microscopy" *Opt. Express* **14**(23), 11204-11214 (2006).
14. J.-X. Cheng, Y. K. Jia, G. Zheng, and X. S. Xie, "Laser-scanning coherent anti-Stokes Raman scattering microscopy and applications to cell biology," *Biophys. J.* **83**, 502-509 (2002).
15. A. M. Weiner, "Femtosecond pulse shaping using spatial light modulators," *Rev. Sci. Instrum.* **71**(5), 1929 (2000).
16. J. W. Chan, D. S. Taylor, and D. L. Thompson, "The effect of cell fixation on the discrimination of normal and leukemia cells with laser tweezers Raman spectroscopy," *Biopolymers* **91**(2), 132-139 (2008).